INTER-RELATIONS OF DOMAIN ORIENTATION AND PIEZOELECTRIC PROPERTIES IN COMPOSITES BASED ON RELAXOR-FERROELECTRIC SINGLE CRYSTALS

V. YU. TOPOLOV,[1,*] C. R. BOWEN[2] AND A. V. KRIVORUCHKO[3]

[1] Department of Physics, Southern Federal University, 344090 Rostov-on-Don, Russia

[2] Materials Research Centre, Department of Mechanical Engineering, University of Bath, BA2 7AY Bath, United Kingdom

[3] Don State Technical University, 344000 Rostov-on-Don, Russia

This paper results on a comparative study of 2–2 relaxor-ferroelectric single crystal / polymer composites. Examples of the hydrostatic piezoelectric performance are discussed for 2–2 composites based on [011]-poled Mn-modified $0.26Pb(In_{1/2}Nb_{1/2})O_3$–$0.42Pb(Mg_{1/3}Nb_{2/3})O_3$–$0.32PbTiO_3$ single crystals at a molar Mn concentration in the range of 1–5 mol. %. High piezoelectric activity of the aforementioned single crystals and rotations of the main crystallographic axes in the single-crystal layers of the composite lead to large values of hydrostatic piezoelectric coefficients d_h^*, g_h^* and e_h^*, squared figure of merit $d_h^* g_h^*$ and electromechanical coupling factor k_h^*. A rotation mode that leads to a weakening of the piezoelectric activity related to the piezoelectric coefficient $d_{32} < 0$ is important to achieve a range of large hydrostatic parameters, e.g., $d_h^* \approx$ (300–350) pC / N, $g_h^* \sim 100$ mV·m / N, $e_h^* \approx$ (21–23) C / m^2, $d_h^* g_h^* \sim (24–30)\cdot 10^{-12}$ Pa^{-1}, and $k_h^* \approx 0.30$. In contrast to $d_h^* g_h^*$, higher values of $d_{33}^* g_{33}^* \sim 10^{-10}$ Pa^{-1} are achieved at the longitudinal piezoelectric effect. The results obtained in this piezoelectric composite system are interpreted by taking into account the orientation of 71° ferroelectric domains in the single-crystal layers.

Keywords: Composite; Ferroelectric; Crystallographic orientation; Anisotropy; Hydrostatic piezoelectric response

PACS: 77.65.-j: Piezoelectricity and electromechanical effects; 77.84.Lf: Composite materials; 77.84.-s: Dielectric; piezoelectric; ferroelectric; and antiferroelectric materials

* Corresponding author. E-mail: vutopolov@sfedu.ru

1. Introduction

Composites based on domain-engineered single crystals (SCs) of perovskite-type relaxor-ferroelectric solid solutions of $(1 - x)Pb(Mg_{1/3}Nb_{2/3})O_3–xPbTiO_3$ (PMN–*x*PT), $(1 - x)Pb(Zn_{1/3}Nb_{2/3})O_3–xPbTiO_3$ (PZN–*x*PT) and $xPb(In_{1/2}Nb_{1/2})O_3–yPb(Mg_{1/3}Nb_{2/3})O_3–(1 - x - y)PbTiO_3$ (*x*PIN–*y*PMN–*z*PT) are modern piezo-active materials [1–4] and are of interest as piezoelectric elements of transducers, sensors, hydrophones, acoustic antennae, etc. Interest in these materials originates from the outstanding electromechanical properties of the aforementioned SCs with compositions near the morphotropic phase boundary. As a consequence, many effective performance parameters of the composites based on these SCs are significantly larger [3, 5] than those in the conventional ceramic / polymer composites [6] with the same microgeometry. A potential mechanism for improving the effective parameters of the SC / polymer composites is related to optimising the orientation of the main crystallographic axes [4] in the SC component. This orientation influences the piezoelectric effect and anisotropy of the electromechanical properties of the composite. A study of the orientation effects in composites with 1–3 [7], 2–2 [8, 9] and 1–0–3 [10] connectivity patterns highlights the important link between the electromechanical properties of the anisotropic SC with a specific orientation of its crystallographic axes and the composite system as a whole. Among the aforementioned composite connectivity patterns, the 2–2 connectivity system seems to be the most simple in the microgeometric sense and is of interest due to its hydrostatic piezoelectric performance [4–6, 8, 9]. A 2–2 composite represents a system of layers of two types (e.g., SC and polymer) that are alternating along the co-ordinate axis.

Our current study is concerned with piezo-active 2–2 composites based on domain-engineered Mn-modified *x*PIN–*y*PMN–*z*PT SCs. The aim of the present paper is to examine the role of domain orientations in the SC component and the related orientation effect in forming the piezoelectric response and hydrostatic parameters of the 2–2 SC / polymer composite. In work [11] Mn-modified SCs with a nominal starting composition of 0.26PIN–0.42PMN–0.32PT taken near the morphotropic phase boundary were grown at a molar concentration of Mn in the range of 1–5 mol. %. Full sets of electromechanical constants were

measured for two sections of the 0.26PIN–0.42PMN–0.32PT:Mn SC poled along $[011]_C$ of the perovskite (or cubic) unit cell (Table 1). A composition of the *SC* ?*section A?* is far away from the nominal morphotropic phase boundary of the *x*PIN–*y*PMN–*z*PT solid solutions. A composition of the *SC section B* is chosen close to the morphotropic phase boundary. The $[011]_C$-poled A and B SCs are characterised by two types of domains of a rhombohedral ferroelectric phase, so that the macroscopic *mm*2 symmetry is observed at the room temperature. The main crystallographic axes in the polydomain state are oriented [11] as follows: X || $[0\bar{1}1]_C$, Y || $[100]_C$ and Z || $[011]_C$, and the average spontaneous polarisation vector of the SC is $\boldsymbol{P}_s^{(1)}$ || Z. In a case of equal volume fractions of the domains of the rhombohedral phase, we assume that their spontaneous polarisation vectors $\boldsymbol{P}_{s,k}$ are oriented as follows: $\boldsymbol{P}_{s,1}$ || $[\bar{1}11]_C$ (the first domain type) and $\boldsymbol{P}_{s,2}$ || $[111]_C$ (the second domain type). It should be added that the Curie temperature varies from approximately 461 K (A SC) to 470 K (B SC). Rhombohedral-monoclinic and monoclinic-tetragonal phase transitions are observed in the A SC at 403 K and 436 K, respectively. In the B SC the rhombohedral-monoclinic and monoclinic-tetragonal phase transitions are observed at 379 K and 394 K, respectively [11].

2. Model Concepts and Averaging Procedures

We will study the piezoelectric performance and related parameters of a 2–2 parallel-connected SC / polymer composite with a regular distribution of layers on the OX_1 direction (Fig. 1). The SC and polymer layers are assumed to be distributed continuously over the OX_2 and OX_3 directions. The relation between the spontaneous polarisation vectors $\boldsymbol{P}_{s,k}$ of domain types and the spontaneous polarisation vector $\boldsymbol{P}_s^{(1)}$ of the polydomain SC layer is shown in the inset of Fig. 1. The polymer layers of the 2–2 composite are piezo-passive.

Hereafter we consider a rotation of the main crystallographic axes X, Y and Z in each polydomain SC layer around one of the co-ordinate axes, namely, along OX_1 || X (rotation angle α, α-mode), OX_2 || Y (rotation angle β, β-mode) or OX_3 || Z (rotation angle γ, γ-mode). Tensors

of the piezoelectric coefficients $d_{ij}^{(1)}$, elastic compliances $s_{ab}^{(1),E}$ and dielectric permittivities $\varepsilon_{ipp}^{(1),\sigma}$ of the SC component are determined [9] using elements of a relevant rotation matrix.

The effective electromechanical properties and other parameters of the 2–2 composite are evaluated using the complete sets of electromechanical constants of components. We consider polyurethane as a piezo-passive polymer component with known elastic and dielectric constants [12]. The electromechanical properties of the *n*th component of the composite in the ($X_1X_2X_3$) system (Fig. 1) are given by the 9 × 9 matrix

$$|| C^{(n)} || = \begin{pmatrix} \left\| s^{(n),E} \right\| & \left\| d^{(n)} \right\|^T \\ \left\| d^{(n)} \right\| & \left\| \varepsilon^{(n),\sigma} \right\| \end{pmatrix}, \qquad (1)$$

where $n = 1$ is related to SC, $n = 2$ is related to polymer, and superscript T denotes the transposed matrix. A procedure for averaging the electromechanical properties is performed taking into consideration nine boundary conditions [3, 4] for electric and mechanical fields in the adjacent layers of the composite sample. These boundary conditions at x_1 = const (see Fig. 1) involve the continuity of three normal components of the mechanical stress (i.e., σ_{11}, σ_{12} and σ_{13}), three tangential components of the mechanical strain (i.e., ξ_{22}, ξ_{23} and ξ_{33}), one normal component of the electric displacement (i.e., D_1), and two tangential components of the electric field (i.e., E_2 and E_3). Following this procedure for averaging, we represent the effective electromechanical properties of the 2–2 composite [3] as

$$|| C^* || = [|| C^{(1)} ||\cdot|| M || m + || C^{(2)} || (1 - m)] [|| M || m + || I || (1 - m)]^{-1}. \qquad (2)$$

The form of the 9 × 9 matrix || C^* || from Eq. (2) is similar to the form of the matrix from Eq. (1). In Eq. (2) || M || is the matrix that describes the aforementioned boundary conditions at x_1 = const, || I || is the identity matrix, m is the volume fraction of the SC, and || $C^{(n)}$ || is taken from Eq. (1). Thus, || C^* || from Eq. (2) comprises the full set of the effective electromechanical properties of the 2–2 composite, namely, elastic compliances at E = const s_{ab}^{*E}, piezoelectric coefficients d_{ij}^* and dielectric permittivities at σ = const $\varepsilon_{fh}^{*\sigma}$. Taking into account three different

rotation modes, we consider $\| C^* \| = \| C^*(m, \alpha) \|$, $\| C^* \| = \| C^*(m, \beta) \|$ or $\| C^* \| = \| C^*(m, \gamma) \|$. Hereby it should be added that $\| C^* \|$ from Eq. (2) is determined in the longwave approximation [3], i.e., the wavelength of the external acoustic field is assumed to be much greater than the width of each layer of the composite sample (Fig. 1). At $\alpha = \beta = \gamma = 0°$ the main crystallographic axes in each SC layer are oriented as described in Section 1.

3. Hydrostatic Parameters

Taking into account the aforementioned rotation modes, we analyse the hydrostatic piezoelectric response of the 2–2 composite based on either the A SC or B SC. Undoubtedly, knowledge of the hydrostatic parameters [3, 5, 6, 12] and their extreme values is of importance for materials selection for hydroacoustic and other piezotechnical applications. Among these parameters, we consider the hydrostatic piezoelectric coefficients

$$d_h^* = d_{31}^* + d_{32}^* + d_{33}^*,\ g_h^* = g_{31}^* + g_{32}^* + g_{33}^* \text{ and } e_h^* = e_{31}^* + e_{32}^* + e_{33}^*, \tag{3}$$

squared hydrostatic figure of merit

$$(Q_h^*)^2 = d_h^*\, g_h^* \tag{4}$$

and hydrostatic electromechanical coupling factor (ECF)

$$k_h^* = d_h^* / \sqrt{s_h^{*E} \varepsilon_{33}^{*\sigma}}\ . \tag{5}$$

The piezoelectric coefficients g_{ij}^* and e_{ij}^* from Eqs. (3) are evaluated using relations [13] $d_{fp}^* = \varepsilon_{fk}^{*\sigma}\, g_{kp}^* = e_{fq}^*\, s_{qp}^{*E}$, and d_{fp}^*, $\varepsilon_{fk}^{*\sigma}$ and s_{qp}^{*E} are taken from $\| C^* \|$ in Eq. (2). The hydrostatic compliance s_h^{*E} from Eq. (5) is defined [12] as $s_h^{*E} = \sum_{a=1}^{3} \sum_{b=1}^{3} s_{ab}^{*E}$. Eqs. (3) and (5) are valid for a case when electrodes applied to the composite sample are parallel to the (X_1OX_2) plane shown in Fig. 1. The hydrostatic piezoelectric coefficients from Eqs. (3) characterise a measure of the activity and sensitivity of the composite under hydrostatic loading. $(Q_h^*)^2$ from Eq. (4) describes the hydrophone signal-to-noise ratio and piezoelectric sensitivity [3]. k_h^* from Eq. (5) is used to evaluate the transducer efficiency under hydrostatic loading [3, 4, 12].

By taking into account a symmetry of the components and the periodic structure of the 2–2 composite (Fig. 1), one can state the periodicity of the orientation dependence of the hydrostatic parameters Π_h^* from Eqs. (3)–(5). For instance, for the aforementioned domain orientations (see inset in Fig. 1) and three rotation modes, conditions

$$X^*(m, \alpha) = X^*(m, 180° - \alpha),\ X^*(m, \beta) = -X^*(m, 180° - \beta) \text{ and } X^*(m, \gamma) = X^*(m, 180° \pm \gamma) \quad (6)$$

hold, where X^* are the effective piezoelectric coefficients, d_h^*, g_h^* and e_h^* from Eqs. (3), and k_h^* from Eq. (5). Based on Eqs. (6), one can state that conditions

$$[Q_h^*(m, \alpha)]^2 = [Q_h^*(m, 180° - \alpha)]^2,\ [Q_h^*(m, \beta)]^2 = [Q_h^*(m, 180° - \beta)]^2 \text{ and } [Q_h^*(m, \gamma)]^2 = [Q_h^*(m, 180° \pm \gamma)]^2 \quad (7)$$

are valid.

4. Rotation Modes, Effective Parameters and Domain Orientations

Changes in the orientation of the main crystallographic axes X, Y and Z of the SC component (see inset in Fig. 1) result in changes in the orientation of the 71° domains therein with respect to the co-ordinate system ($X_1X_2X_3$). These changes in domain orientation influence the piezoelectric coefficients of the SC component and composite in different ways, depending on the rotation mode and will now be discussed.

In a case of the α-mode [need to clarify what is alpha-mode] the composite is characterised by relatively small values of the hydrostatic parameters from Eqs. (3)–(5). For example, $d_h^*(m, \alpha)$ has minimum at α = const in the range from 0° to 90°, and $|\min d_h^*(m, \alpha)| < d_h^*(1, \alpha)$. At α = 90° we obtain $d_{3j}^* = 0$ due to the symmetrical arrangement of the domains with respect to the (X_1OX_2) plane (see Fig. 1). At the α-mode we observe the rotation of the spontaneous polarisation vector $\boldsymbol{P_s}^{(1)}$ of the polydomain SC in the (X_2OX_3) plane that is parallel to the composite interfaces, and such a rotation leads to relatively large piezoelectric coefficients and

related hydrostatic parameters at $\alpha \approx 0°$ only. This is a result of the considerable anisotropy of the piezoelectric and elastic properties of the $[011]_C$ SC (see Table 1).

The β-mode means that the spontaneous polarisation vector $\boldsymbol{P_s^{(1)}}$ crosses the interfaces in the composite sample (Fig. 1), and the domain arrangement is more favourable to achieve a pronounced piezoelectric effect. However the piezoelectric coefficient $d_h^*(m, \beta)$ is relatively small due to contributions from d_{31}^* and d_{32}^* at sgn d_{32}^* = –sgn d_{31}^*: for both the A SC- and B SC-based composites max $d_h^*(m, \beta) < d_h^{(1)}$ at $0° < \beta < 90°$, and $d_h^* = 0$ at $\beta = 90°$. The small values of d_h^* in comparison to $d_h^{(1)}$ lead to small values of the remaining hydrostatic parameters from Eqs. (3)–(5).

The γ-mode [need to explain gamma mode] enables us to attain an effective re-distribution of the piezoelectric activity of SC on the non-polar OX_1 and OX_2 directions. Data from Table 1 suggest that for the A and B SCs the condition sgn $d_{32}^{(1)}$ = –sgn $d_{31}^{(1)}$ is valid. The rotation of the main crystallographic axes of the SC around the poling axis OX_3 leads to considerable changes in d_{31}^* and d_{32}^* and, therefore, contributions from d_{31}^* and d_{32}^* into d_h^* from Eqs. (3) influence the complete system of the hydrostatic parameters from Eqs. (3)–(5). Since the spontaneous polarisation vector $\boldsymbol{P_s^{(1)}}$ of the polydomain SC remains parallel to the poling axis OX_3, no appreciable change in the longitudinal piezoelectric effect of the composite is expected.

In the case of the γ-mode we obtain a set of large values of the hydrostatic parameters from Eqs. (3)–(5), especially at $\gamma = 45°$–$90°$. Examples of local maxima of these parameters are shown in Fig. 2. Graphs in Fig. 2 contain data on $(\Pi_h^*)_m = \max \Pi_h^*(m, \gamma)|_{\gamma = \text{const}}$ and relevant volume fractions of SC. These volume fractions are termed m_d for $(d_h^*)_m$, m_e for $(e_h^*)_m$, m_g for $(g_h^*)_m$, m_Q for $[(Q_h^*)_m]^2$, and m_k for $(k_h^*)_m$. For instance, $(d_h^*)_m$ (curves 1 and 3 in Fig. 2a) is achieved at m_d that undergo changes (see curves 2 and 4 in Fig. 2a) at the rotation of the main crystallographic axes or at the change in γ. Curves 3 and 4 in Fig. 2a were built in the γ range where $(d_h^*)_m$ is

observed, and at smaller γ values d_h^* is characterised by either a monotonic volume-fraction dependence or a non-monotonic with a slight $\min d_h^*$ [do not understand this]. It is possible that at $\gamma < 45°$, the is an intricate competition between d_{3j}^* in Eqs. (3) and $\min d_h^*$ appears to obey the condition $|\min d_h^*(m, \gamma)| < d_h^{(1)}$. This is due to the important piezoelectric and elastic anisotropy of the A and B SCs. Our evaluations based on data from Table 1 lead to $d_h^{(1)}$ = 65 pC / N and 153 pC / N for the A SC and B SC, respectively.

Local maxima of g_h^* are achieved at fairly small volume fractions m_g (curves 2 and 4 in Fig. 2b) in comparison to the volume fractions m_d and m_e (curves 2 and 4 in Figs. 2a and 2c). Such a behaviour is typical of the 2–2 composite system [3, 4] irrespective of its piezoelectric component, either a relaxor-ferroelectric SC with a high piezoelectric activity or a poled ferroelectric ceramic with a lower piezoelectric activity. Replacing m_g with a larger volume fraction m, we observe relatively large values of g_h^* at m < 20%. For instance, at m = 10% in the A SC-based composite, we obtain g_h^* ~ 100 mV·m / N in a wide range of γ (Table 2). We choose m = 10%, since in a vicinity of this value, local maxima of $(Q_h^*)^2$ and k_h^* are observed (Figs. 2d and 2e), and a composite sample can be manufactured at m = 10% and larger values without technological challenges achieving such as small volume fraction. Based on data from Table 1, we obtain $g_h^{(1)}$ = 2.28 mV·m / N for the A SC. Comparing this value to g_h^* at γ = 90° (see Table 2), we can observe that the hydrostatic piezoelectric sensitivity increases by ca. 63 times. This increase is due to the large piezoelectric coefficient d_h^* and the relatively small dielectric permittivity $\varepsilon_{33}^{*\sigma}$ of the 2–2 composite. The large values of g_h^* ~ 100 mV·m / N are also achieved in the B SC-based composite at $g_h^{(1)}$ = 4.91 mV·m / N for the B SC.

Fig. 2c shows that large values of $(e_h^*)_m$ are related to m_e = 80–90%. A small difference between $(e_h^*)_m$ related to the A SC-based and B SC-based composites (see curves 1 and 3 in Fig. 2c) is due to the influence [3, 4] of the elastic properties of the composite on the piezoelectric

coefficients e_{3j}^{*}, especially at large volume fractions of SC. It should be highlighted that there is a considerable increase of e_h^{*} in both the composites in a wide volume-fraction range. As follows from our evaluations by using data from Table 1, the hydrostatic piezoelectric coefficients $e_h^{(1)}$ = 7.15 C / m^2 and 7.01 C / m^2 are related to the A SC and B SC, respectively.

In contrast to $(e_h^{*})_m$, local maxima of $(Q_h^{*})^2$ from Eq. (4) are observed at smaller volume fractions (Fig. 2d). This is due to the active influence of the dielectric properties of the composite which is compromise between decreasing g_h^{*} and increasing d_h^{*} at $m \approx 10\%$. Large values of $[(Q_h^{*})_m]^2$ can be observed for both the composites at $\gamma = 75°–90°$ (see curves 1 and 3 in Fig. 2d). At such an orientation of the main crystallographic axes, as with d_h^{*} and g_h^{*}, the piezoelectric response concerned with $d_{32}^{(1)} < 0$ is weakened because of the interfaces of the composite (Fig. 1). We add for comparison that values of $(Q_h^{(1)})^2 = 0.148 \cdot 10^{-12}$ Pa^{-1} (A SC) and $0.751 \cdot 10^{-12}$ Pa^{-1} (B SC) are obtained from data in Table 1. Despite the large difference between these values, we do not see a large difference between curves 1 and 3 in Fig. 2d. This can be explained by taking into consideration the dielectric permittivity of the composite at various γ angles.

In Fig. 2e we can observe changes in the hydrostatic electromechanical coupling factor k_h^{*} from Eq. (5). In general this behaviour is consistent with changes in d_h^{*} on varying the rotation angle γ. At $\gamma = 75°–90°$ a small difference between k_h^{*} for the A SC-based and B SC-based composites is observed despite the large difference between the aforementioned $d_h^{(1)}$ values of these SCs. The similar behaviour of k_h^{*} for the two SC type is related to the role of the dielectric permittivity of the composite at volume fractions $m \approx 10\%$. The orientation effect enables us to increase k_h^{*} in the A SC-based composite by about 2.3 times in comparison to $k_h^{(1)}$ of the SC component. In the case of the B SC-based composite, k_h^{*} increases slightly in comparison to $k_h^{(1)}$. This is due to the larger hydrostatic elastic compliance s_h^{*E} and dielectric permittivity $\varepsilon_{33}^{*\sigma}$ of the

composite at $m \approx 10\%$: Eq. (5) suggests that s_h^{*E} and $\varepsilon_{33}^{*\sigma}$ strongly influence k_h^*, especially at $m \ll 1$.

Fig. 3 shows changes in $(Q_h^*)^2$ near the absolute maximum point at the γ-mode. It is seen that variations of the volume fraction of SC m by about 5% do not lead to a considerable increase of $(Q_h^*)^2$ at various γ angles, and this circumstance facilitates a selection of composites for hydroacoustic applications concerned with large values of $(Q_h^*)^2$, g_h^* etc. [3–6].

It is important to compare $(Q_h^*)^2$ (Figs. 2d and 3) to the squared figure of merit

$$(Q_{33}^*)^2 = d_{33}^* g_{33}^* \qquad (8)$$

that is concerned with the longitudinal piezoelectric response of the composite. Local maxima $[(Q_{33}^*)_m]^2 = \max [Q_{33}^*(m, \gamma)]^2|_{\gamma = \text{const}}$ and relevant volume fractions of SC m_{Q33} (Fig. 4) are also subject to an orientation effect despite the piezoelectric response along the rotation axis OX_3 (Fig. 1). Such a behaviour is concerned with changes in the elastic and dielectric properties at the γ-mode, especially at relatively small volume fractions m_{Q33} (see curves 2 and 4 in Fig. 4). We remind that the piezoelectric coefficient d_{33}^* from Eq. (8) increases depending on the elastic properties of the polymer component [3, 4]. In contrast to d_{33}^*, the piezoelectric coefficient g_{33}^* from Eq. (8) passes the maximum point that strongly depends on the elastic and dielectric properties of the polymer component [3, 4]. Curves 1 and 3 in Fig. 4 show that $[(Q_{33}^*)_m]^2$ is achieved at $\gamma = 45°$ and differs from $[(Q_h^*)_m]^2$ in Fig. 2d. The orientation of the main crystallographic axes at $\gamma = 45°$ corresponds to the domain arrangement wherein one of the 71° domains is located at the interface $x_1 = \text{const}$ between the SC and polymer layers (Fig. 1). At such a domain orientation the equality of the piezoelectric coefficients $d_{31}^{(1)}$ and $d_{32}^{(1)}$ holds for SC and leads to absolute max $[(Q_{33}^*)^2]$ of the composite at the γ-mode.

The maximum values of d_h^*, g_h^* and $(Q_h^*)^2$ of the studied 2–2 composites highlight their advantages over conventional 2–2 PZT-type ferroelectric ceramic / polymer composites [6]. The

values of d_h^*, g_h^*, e_h^*, $(Q_h^*)^2$, and $(Q_{33}^*)^2$ (Figs. 2–4 and Table 2) are comparable to those found for 1–3 and 2–2 composites based on either PMN–*x*PT or PZN–*x*PT SCs [1–5, 8, 9]. It is remarkable that values of the piezoelectric coefficients g_{3j}^* and squared figure of merit $(Q_h^*)^2$ remain large at deviations from the optimum volume fraction by a few percent.

5. Conclusions

The present paper has been devoted to the orientation effect in 2–2 relaxor-ferroelectric SC / polymer composites. Among the potential SC components with a high piezoelectric activity, two related compositions of 0.26PIN–0.42PMN–0.32PT:Mn (A and B SCs at the molar concentration of Mn from 1 to 5%) have been examined. The A and B SCs poled along $[011]_C$ of the perovskite unit cell are of interest due to the anisotropy of their electromechanical properties (Table 1). Examples of the orientation effect, maxima of the hydrostatic parameters (Figs. 2 and 3) and squared figure of merit $(Q_{33}^*)^2$ (Fig. 4) have been interpreted by taking into account the orientation of the domains in the SC layer and its electromechanical constants on poling along $[011]_C$. It is clear that the higher piezoelectric activity of the B SC do not always result in the largest parameters in the related 2–2 composite at variations of the volume fraction of SC and changes in the orientation of the main crystallographic axes. The *γ*-mode associated with the rotation of the main crystallographic axes around OX_3 (Fig. 1) is of interest due to largest values of the studied hydrostatic parameters from Eqs. (3)–(5). The *γ*-mode enables us to maintain the orientation of the spontaneous polarisation vector $\boldsymbol{P_s^{(1)}} \parallel OX_3$ in the SC layer and to effectively influence the balance of the piezoelectric coefficients of the composite at sgn $d_{32}^{(1)}$ = –sgn $d_{31}^{(1)}$ in its SC component.

The results shown in the present paper highlight the high performance of the studied 2–2 SC / polymer composites on rotation of the main crystallographic axes and obvious advantages of these composites over the conventional 2–2 ferroelectric ceramic / polymer composites. The large values of d_h^*, e_h^*, g_h^*, $(Q_h^*)^2$, k_h^*, and $(Q_{33}^*)^2$ are achieved at specific orientations of the

main crystallographic axes of SC and due to a specific anisotropy of its elastic and piezoelectric properties. The orientation effect studied in the 2–2 composites with related SC components shows us a way to the large hydrostatic parameters, piezoelectric coefficients and figures of merit which can be used in modern hydroacoustic, piezoelectric energy-harvesting, sensor, and other applications.

Acknowledgements

The authors would like to thank Prof. Dr. A. E. Panich, Prof. Dr. I. A. Parinov and Prof. Dr. A. A. Nesterov (Southern Federal University, Rostov-on-Don, Russia), Prof. Dr. P. Bisegna (University of Rome "Tor Vergata", Italy), and Prof. Dr. M. Lethiecq and Dr. F. Levassort (François Rabelais University, Tours, France) for their continuing interest in the research problems. Special thanks are extended to Prof. Dr. L. N. Korotkov (Voronezh State Technical University, Russia) for his invitation to give a plenary talk on the research results at ISFP-8 (13). Bowen would like to acknowledge funding from the European Research Council under the European Union's Seventh Framework Programme (FP/2007-2013) / ERC Grant Agreement no. 320963 on Novel Energy Materials, Engineering Science and Integrated Systems (NEMESIS).

References

1. K. C. Cheng, H.L.W. Chan, C.L. Choy, Q. Yin, H. Luo, and Z. Yin, Single crystal PMN-0.33PT/epoxy 1–3 composites for ultrasonic transducer applications. *IEEE Trans. Ultrason., Ferroelec., a. Freq. Contr*. **50**, 1177–1183 (2003).

2. F. Wang, C. He, Y. Tang, X. Zhao, and H. Luo, Single-crystal $0.7Pb(Mg_{1/3}Nb_{2/3})O_3$–$0.3PbTiO_3$/epoxy 1–3 piezoelectric composites prepared by the lamination technique. *Mater. Chem. Phys*. **105**, 273–277 (2007).

3. V. Yu. Topolov and C. R. Bowen, *Electromechanical Properties in Composites Based on Ferroelectrics*. London: Springer; 2009.

4. V. Yu. Topolov, P. Bisegna, and C. R. Bowen, *Piezo-active Composites. Piezo-active Composites. Orientation Effects and Anisotropy Factors*. Springer, Berlin Heidelberg; 2014.

5. L. Li, S. Zhang, Z. Xu, X. Geng, F. Wen, J. Luo, and T. R. Shrout, Hydrostatic piezoelectric properties of [011] poled $Pb(Mg_{1/3}Nb_{2/3})O_3$–$PbTiO_3$ single crystals and 2–2 lamellar composites. *Appl. Phys. Lett.* **10**4, 032909–5 p. (2014).

6. E. K. Akdogan, M. Allahverdi, and A. Safari A, Piezoelectric composites for sensor and actuator applications. *IEEE Trans. Ultrason., Ferroelec., a. Freq. Contr*. **52**, 746–775 (2005).

7. V. Yu. Topolov, A. V. Krivoruchko, P. Bisegna, and C. R. Bowen, Orientation effects in 1–3 composites based on $0.93Pb(Zn_{1/3}Nb_{2/3})O_3$-$0.07PbTiO_3$ single crystals. *Ferroelectrics* **376**, 140–152 (2008).

8. A. V. Krivoruchko and V. Yu. Topolov, On the remarkable performance of novel 2–2-type composites based on [011] poled $0.93Pb(Zn_{1/3}Nb_{2/3})O_3 - 0.07PbTiO_3$ single crystals. *J. Phys. D: Appl. Phys*. **40**, 7113–7120 (2007).

9. V. Yu. Topolov and A. V. Krivoruchko, Polarization orientation effect and combination of electromechanical properties in advanced $0.67Pb(Mg_{1/3}Nb_{2/3})O_3$-$0.33PbTiO_3$ single crystal / polymer composites with 2–2 connectivity. *Smart Mater. Struct*. **18**, 065011–11 p. (2009).

10. V. Yu. Topolov, C. R. Bowen, P. Bisegna, and A. V. Krivoruchko, New orientation effect in piezo-active 1–3-type composites. *Mater. Chem. Phys.* **151**, 187–195 (2015).

11. X. Huo, S. Zhang, G. Liu, R. Zhang, J. Luo, R. Sahul, W. Cao, and T. R. Shrout, Complete set of elastic, dielectric, and piezoelectric constants of $[011]_C$ poled rhombohedral $Pb(In_{0.5}Nb_{0.5})O_3$-$Pb(Mg_{1/3}Nb_{2/3})O_3$-$PbTiO_3$:Mn single crystals. *J. Appl. Phys*. **113**, 074106–5 p. (2013).

12. L.V. Gibiansky and S. Torquato, On the use of homogenization theory to design optimal piezocomposites for hydrophone applications. *J. Mech. Phys. Solids* **45**, 689–708 (1997).

13. I. S. Zheludev, *Physics of Crystalline Dielectrics. V. 2: Electrical Properties*. New York: Plenum; 1971.

Table 1. Elastic compliances $s_{ab}^{(1),E}$ (in 10^{-12} Pa^{-1}), piezoelectric coefficients $d_{ij}^{(1)}$ (in pC / N) and relative dielectric permittivity $\varepsilon_{pp}^{(1),\sigma}/\varepsilon_0$ of poled A and B SCs components at room temperature

Electrome-chanical constant	$[011]_C$-poled A SC [11]	$[011]_C$-poled B SC [11]
$s_{11}^{(1),E}$	18.0	23.5
$s_{12}^{(1),E}$	–28.0	–39.0
$s_{13}^{(1),E}$	13.1	20.6
$s_{22}^{(1),E}$	68.1	90.4
$s_{23}^{(1),E}$	–39.4	–56.4
$s_{33}^{(1),E}$	30.9	43.8
$s_{44}^{(1),E}$	15.5	16.2
$s_{55}^{(1),E}$	116	189
$s_{66}^{(1),E}$	20.0	21.1
$d_{15}^{(1)}$	2030	2986
$d_{24}^{(1)}$	125	160
$d_{31}^{(1)}$	455	608
$d_{32}^{(1)}$	–1200	–1509
$d_{33}^{(1)}$	810	1053
$\varepsilon_{11}^{(1),\sigma}/\ \varepsilon_0$	4916	6274
$\varepsilon_{22}^{(1),\sigma}/\ \varepsilon_0$	1084	1499
$\varepsilon_{33}^{(1),\sigma}/\ \varepsilon_0$	3213	4523

Table 2. Orientation dependence of piezoelectric coefficients g_{3j}^{*} and g_{h}^{*} (in mV·m / N) of the 2–2 A SC / polyurethane composite at m = 10% and γ-mode

γ, deg	g_{31}^{*}	g_{32}^{*}	g_{33}^{*}	g_{h}^{*}
0	50.3	–301	227	–23.7
15	38.1	–322	270	–13.9
30	–14.1	–248	278	15.9
45	–97.8	–122	281	61.2
60	–180	10.9	277	108
75	–230	96.7	268	135
90	–245	124	265	144

Figure captions to the paper

"Domain Orientations – Piezoelectric Properties Inter-relations in Composites Based on Relaxor-Ferroelectric Single Crystals" by V. Yu. Topolov, C. R. Bowen and A. V. Krivoruchko

Fig. 1. Schematic of the 2–2 SC / polymer composite with parallel-connected layers. ($X_1X_2X_3$) is a rectangular co-ordinate system, m and $1 - m$ are volume fractions of SC and polymer, respectively, $\boldsymbol{P}_s^{(1)}$ is the spontaneous polarisation vector of the SC component. Inset comprises domain orientations in the $[011]_C$-poled SC with the average spontaneous polarisation vector $\boldsymbol{P}_s^{(1)}$. $\boldsymbol{P}_{s,1}$ and $\boldsymbol{P}_{s,2}$ are spontaneous polarisation vectors of several domain types oriented within a cubic cell. X, Y and Z are main crystallographic axes of the polydomain SC.

Fig. 2. Local maxima of hydrostatic parameters from Eqs. (3)–(5) and relevant volume fractions of SC in 2–2 SC / polyurethane composites at the γ-mode.

Fig. 3. Hydrostatic squared figure of merit $(Q_h^*)^2$ near absolute maximum in the 2–2 B SC / polyurethane composite at the γ-mode.

Fig. 4. Local maxima of the squared figure of merit $(Q_{33}^*)^2$ from Eq. (8) and relevant volume fractions of SC in 2–2 SC / polyurethane composites at the γ-mode.

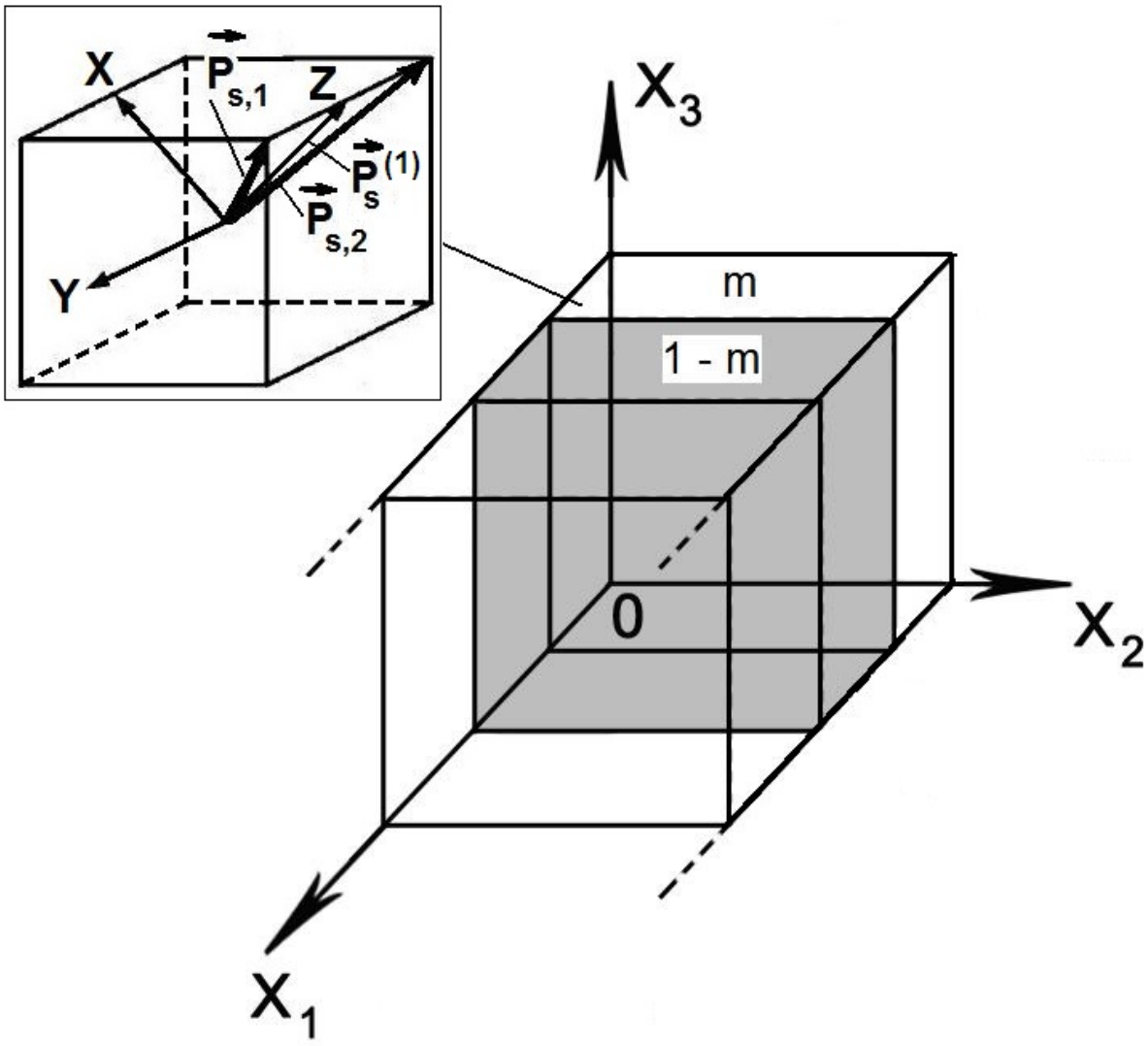

Fig. 1

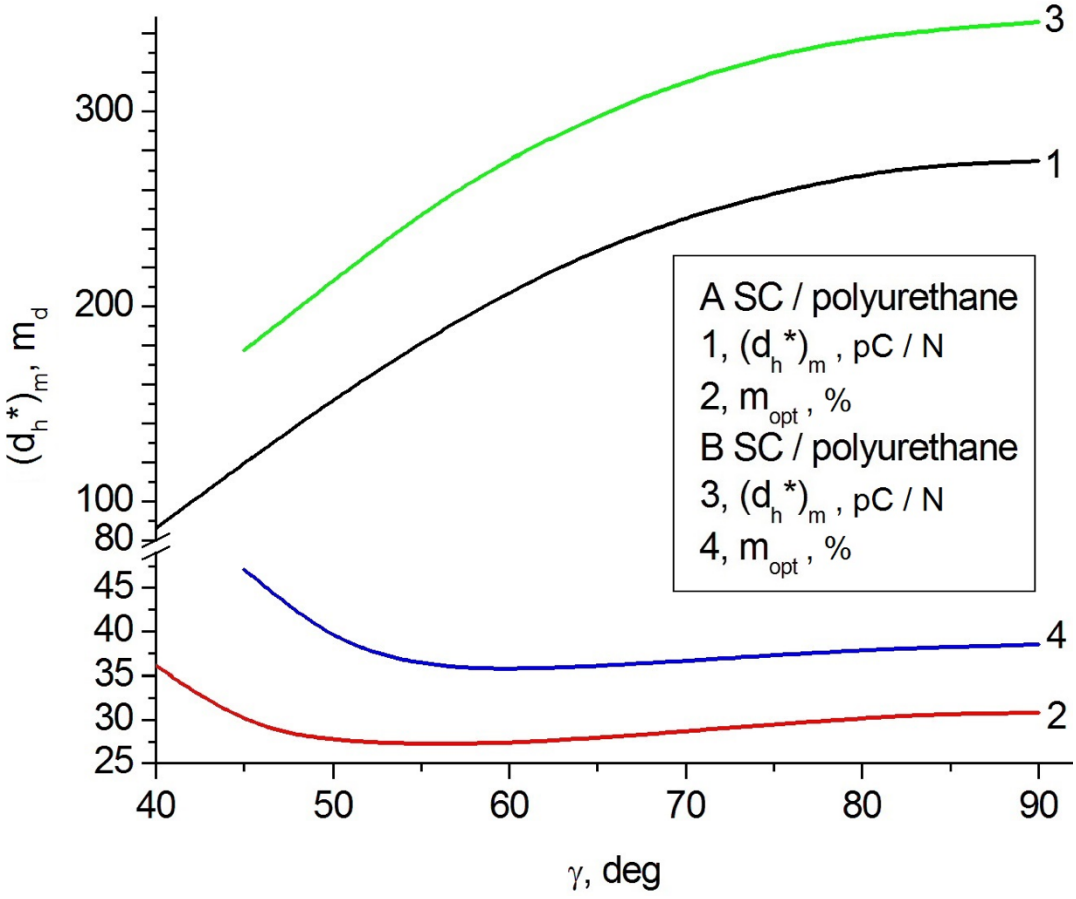

a

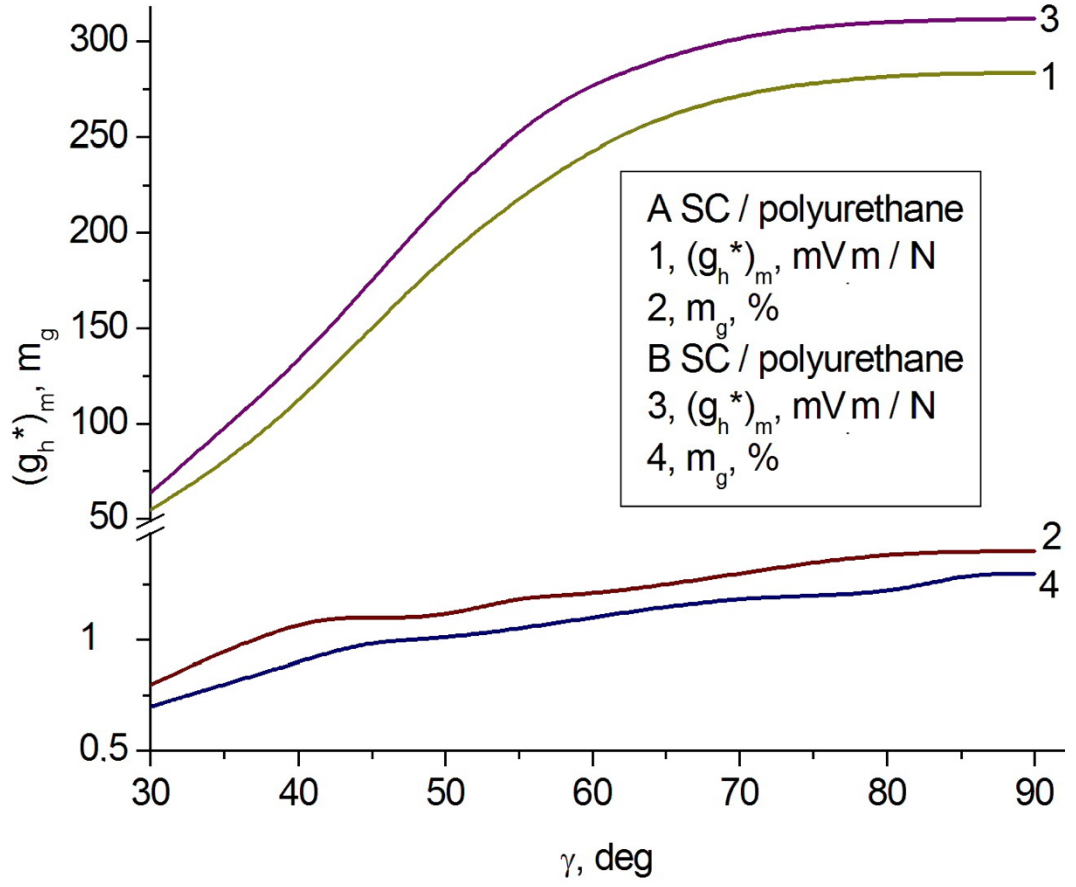

b Fig. 2 (*continued*)

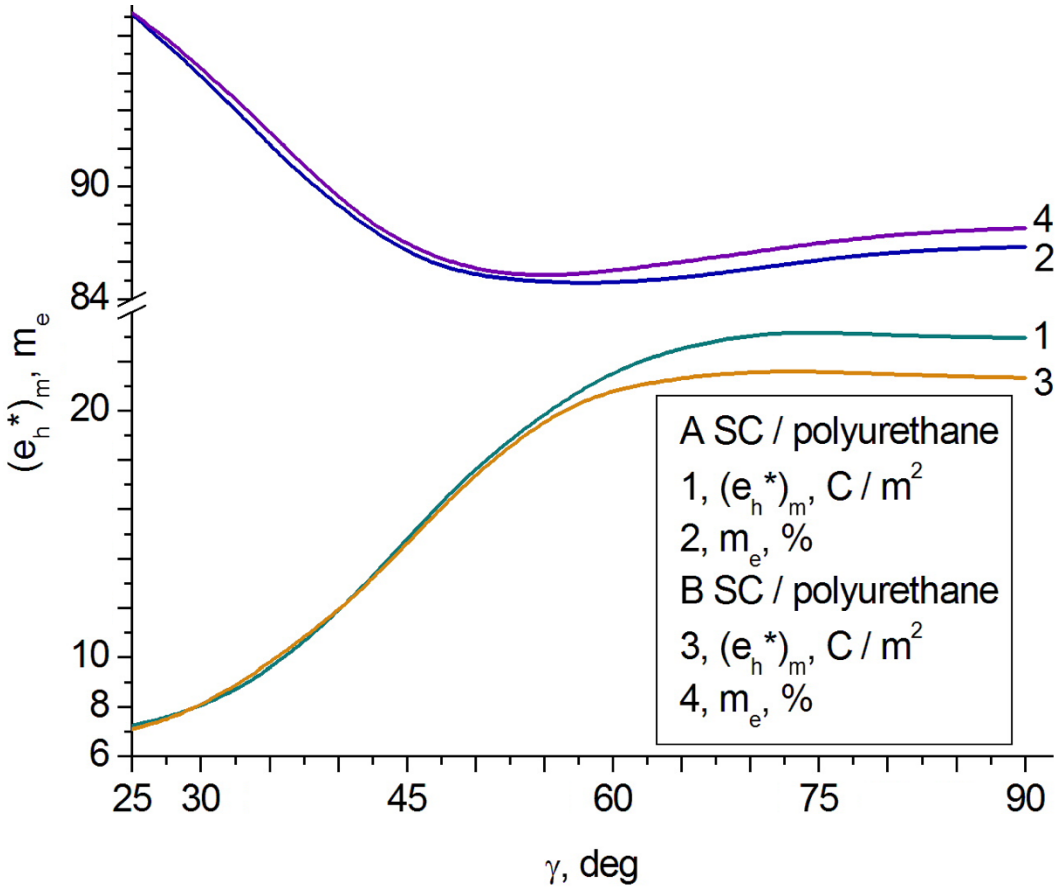

c

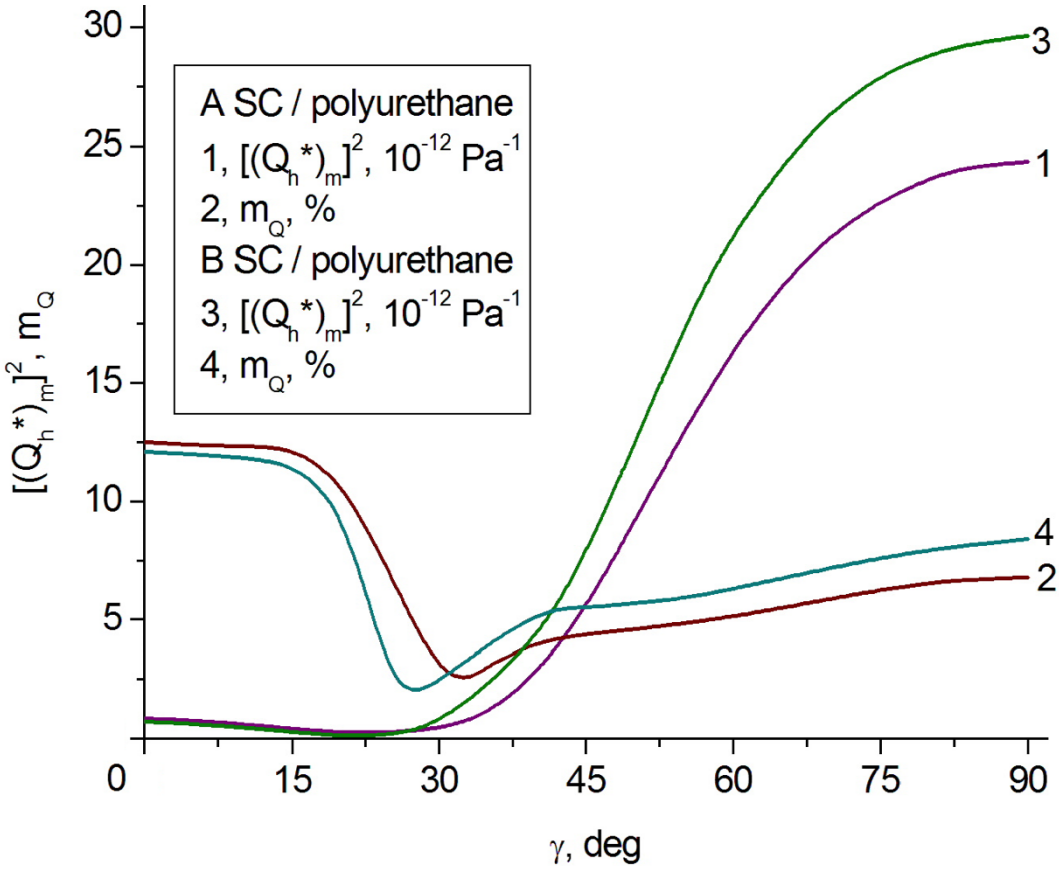

d

Fig. 2 (*continued*)

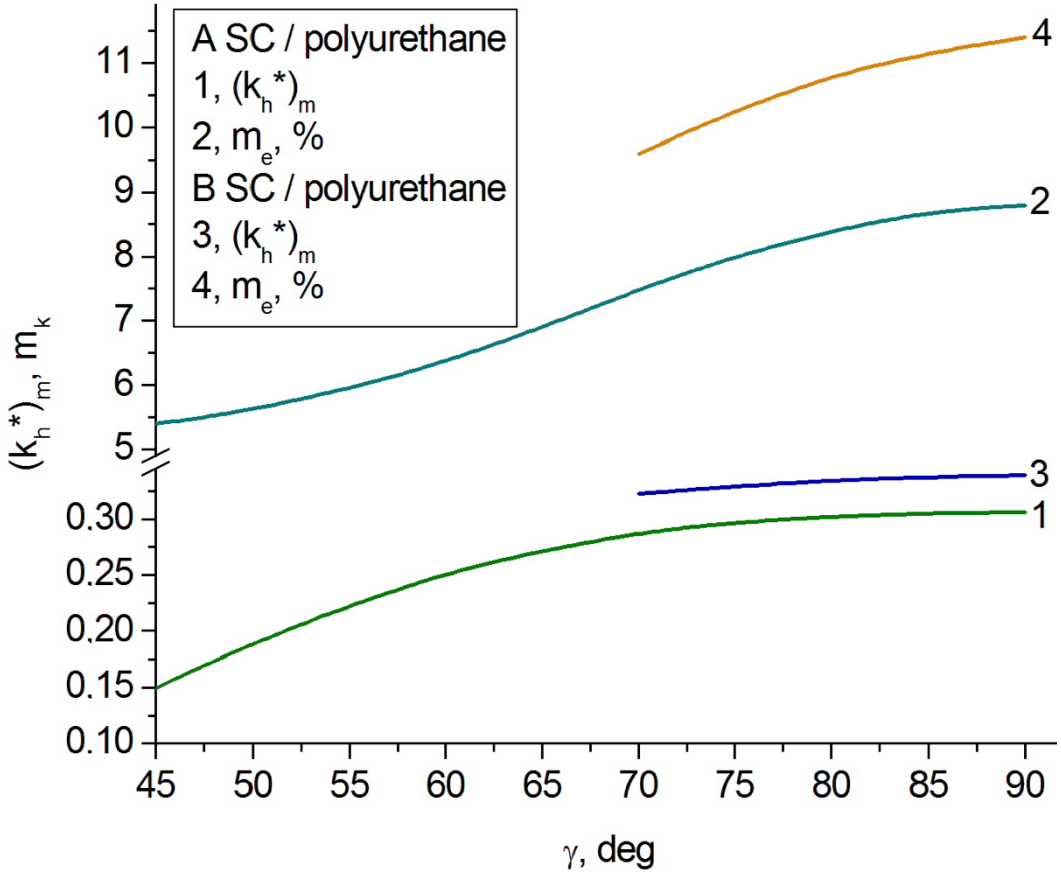
A SC / polyurethane
1, $(k_h^*)_m$
2, m_e, %
B SC / polyurethane
3, $(k_h^*)_m$
4, m_e, %
$(k_h^*)_m$, m_k
γ, deg
1
2
3
4

e

Fig. 2

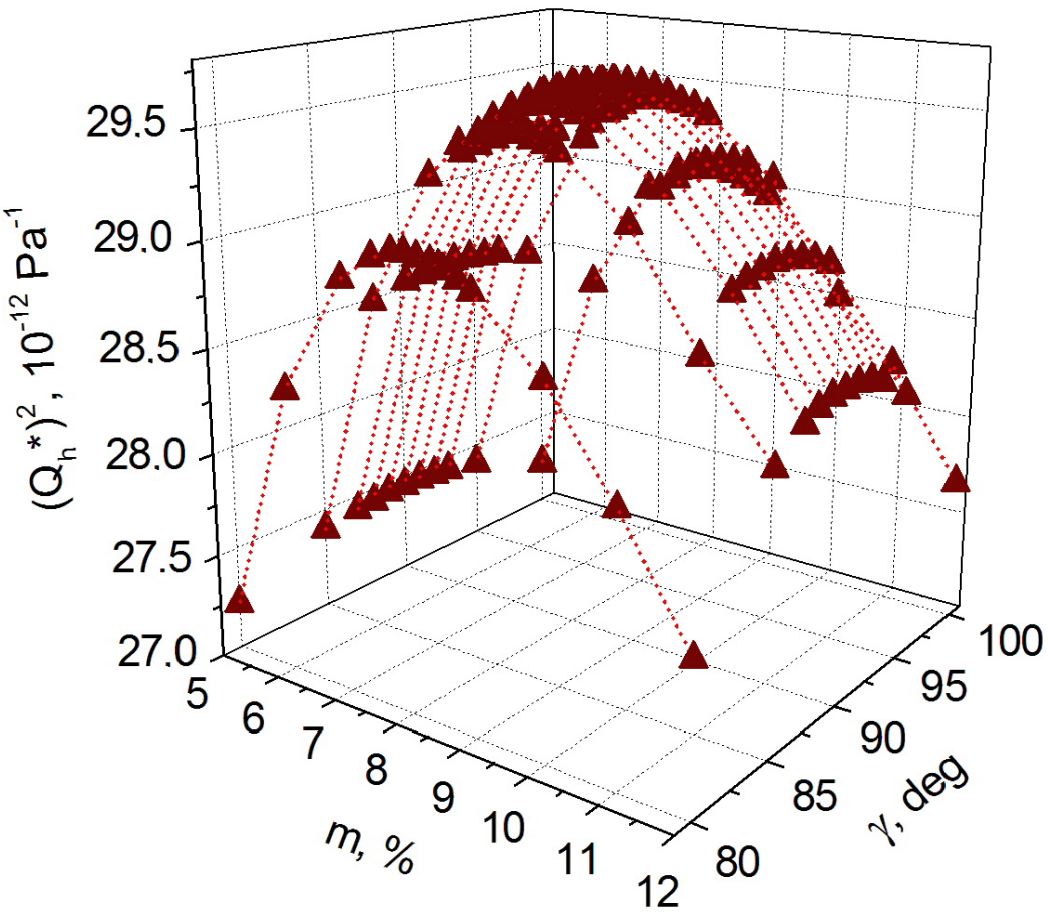
29.5
29.0
28.5
28.0
27.5
27.0
$(Q_h^*)^2$, 10^{-12} Pa^{-1}
5
6
7
8
9
10
11
12
m, %
80
85
90
95
100
γ, deg

Fig. 3

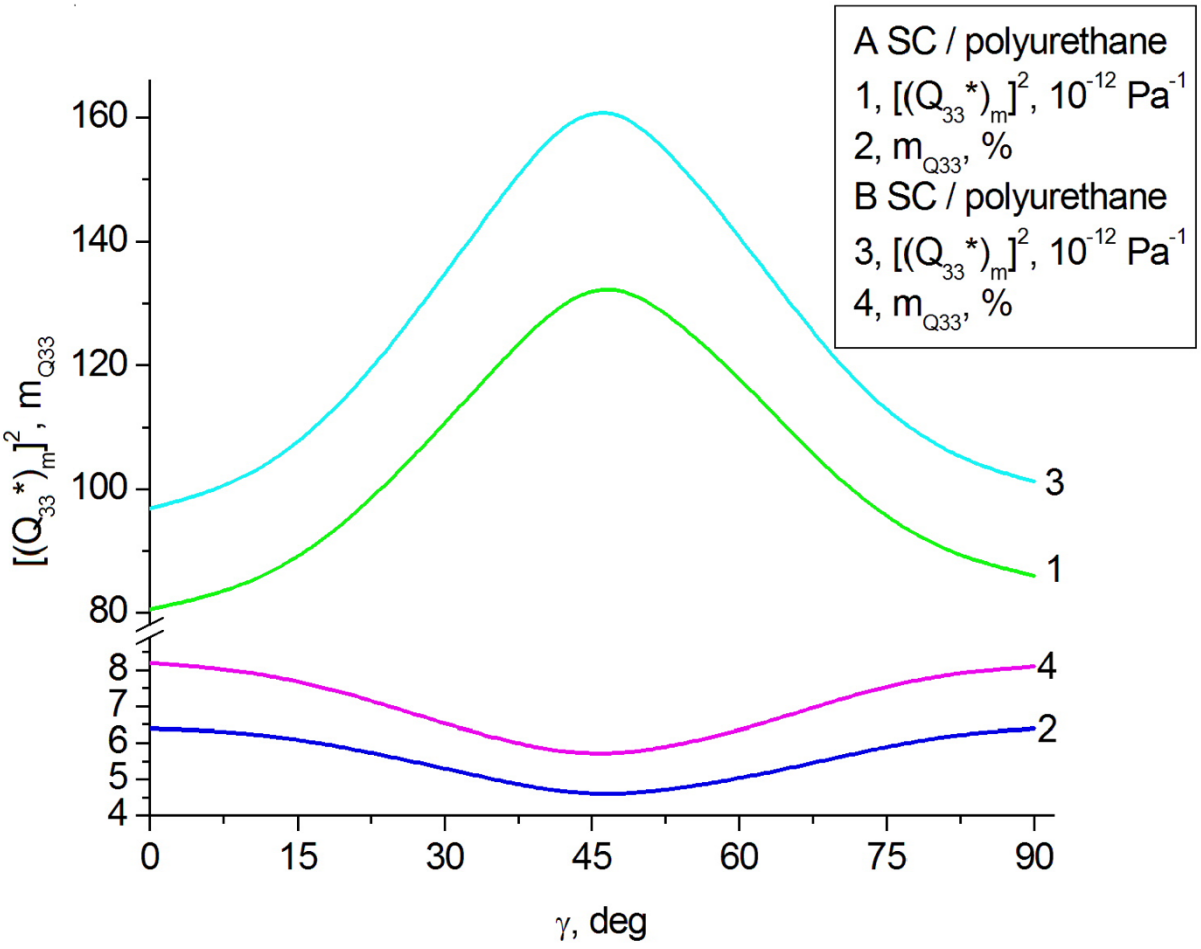
A SC / polyurethane
1, [(Q33*)m]2, 10-12 Pa-1
2, mQ33, %
B SC / polyurethane
3, [(Q33*)m]2, 10-12 Pa-1
4, mQ33, %
[(Q33*)m]2, mQ33
160
140
120
100
80
8
7
6
5
4
0
15
30
45
60
75
90
γ, deg
1
2
3
4

Fig. 4